DRAFT VERSION SEPTEMBER 28, 2017
Typeset using LaTeX **twocolumn** style in AASTeX61

THE MILKY WAY AND SOLAR NEIGHBORHOOD SUPERNOVA RATE: IMPLICATIONS FOR GRAVITATIONAL WAVES PROBES FROM SUPERNOVAE

MADS SØRENSEN,[1,2] CHRISTOPHER LEE FRYER,[3] NICOLE MARIE LLOYD-RONNING,[3] JESS MCIVER,[4] PHILIP MÖSTA,[5] DANIEL HOLZ,[6] AND DUNCAN BROWN[7]

[1]*Observatory of Geneva, University of Geneva, Chemin des Maillattes 51, 1290 Versoix ,Switzerland*
[2]*DARK, Niels Bohr Institute, University of Copenhagen, Juliane Maries vej 31, 2100 Copenhagen, Denmark*
[3]*CCS Division, Los Alamos National Laboratory, Los Alamos, NM 87545, USA*
[4]*California Institute of Technology, Pasadena, CA 91125, USA*
[5]*Department of Astronomy 501 Campbell Hall #3411 University of California at Berkeley Berkeley, CA 94729-3411, USA*
[6]*Enrico Fermi Institute, 5620 S. Ellis Ave, Chicago, IL 60637, USA*
[7]*Department of physics, Syracuse University, Syracuse, NY 13244, USA*

ABSTRACT

We investigate gravitational waves (GWs) as probes of the engine(s) of core collapse (CC) supernovae (SNe) and review current available theorized CCSN engines, to formulate GW toy models that to 0^{th} order, for each CCSN engine is descriptive of the expected signal. Our focus are, explosions due to the convective engine and magnetized rapidly rotating engines.

Since, GW signals from CCSN are only detectable in the very local Universe dominated by the stellar field of the Milky Way (MW) we revisit the SN frequency of the MW, comparing it with solar neighborhood SN activity, from different data sources. In this process, we account for the Sun's MW position and the MW structure. Hence, we estimate the expected waiting time for a CCSN in the MW, observable with present and future GW detections. Our finding, is that the recent 7 historical SNe near the Sun within 1000 yr, was a rare chain of events, most probably only happening once during a million year period. Finally, we also discuss the implications from recent estimates of the Hubble constant, to the MW SN frequency estimates from extragalactic surveys. Potentially, extragalactic surveys overestimate the MW SN frequency by 20%.

Keywords: Supernova: rates, frequencies — The Milky Way: structure — Gravitational waves

1. INTRODUCTION

A supernova (SN), is the end of a stars life, as a fusion reactor. It marks the transition of the star into a Neutron star of a black hole (BH). The transition is observable as a point source as bright as an entire galaxy. Most SN happens because massive stars undergoes a core collapse in which

1. what are supernova?
2. what are gravitational waves?
3. how are the two related?
4. If we have a close enough SN what can we learn about GWs?
5. If we have a close enough SN what can we learn about SN engines?
6. what is "known" about GW signals from supernova?
7. what are the current best bet for a detection rate?

We follow Li et al. (2011a) and assume the Milky Way (MW) is a Sbc type galaxy.

2. SUPERNOVA ENGINES AND GRAVITATIONAL WAVE PRODUCTION

Core-collapse supernovae (CCSN) are powered by the gravitational potential energy released when the core of a massive star collapses to form a neutron star. The onset of collapse occurs when the iron core, supported by electron-degeneracy and thermal pressure, becomes so compact under its own weight that electrons capture onto protons. The subsequent reduction in pressure support compresses the core further, accelerating the electron capture (and dissociation of the iron atoms), and ultimately causing a runaway collapse. This collapse proceeds until the core reaches nuclear densities where nuclear forces and neutron degeneracy pressure halt the collapse, causing the core to bounce. Although the bounce shock stalls, the energy released in the collapse is 30-100 times greater than that needed to explain most supernovae. To revive the shock, the energy above the proto-neutron star (PNS) must tap this energy to overcome the outer layers of the star, collapsing onto the core. However, the details describing exactly how this energy is converted into the explosion energies observed in CCSN remains an active area of research. Two classes of supernova engine use the energy released in the collapse: magnetic-field engines that tap rotational energy and the âĂIJconvective engineâĂİ that relies upon the thermal energy of the collapse.

The current leading CCSN engine is the âĂIJconvective engineâĂİ where convection between the PNS and the stalled shock increases the efficiency at which the thermal energy in the collapse is converted into explosion energy(Herant et al. 1994) **More citations here**. This convection allows heated material at the base of the convective region to rise, converting thermal energy to kinetic energy. It also transports the infalling material from the outer layers of the star to the PNS surface, reducing the pressure that must be overcome at the stalled shock and releasing additional potential energy. This engine provides an explanation for the fact that although nearly 10^{53} erg is released in the collapse, most supernova energies are 10^{51} erg. The convective engine predicted that supernovae would mostly be produced in stars between $8-20\,M_\odot$(Fryer 1999). Initially at odds with observations(Hamuy 2003), this prediction is now confirmed through the observations of supernova progenitors(Smartt 2009). It also predicted a range of compact remnant massesFryer & Kalogera (2001) that, again, was initially at odds with observations arguing for delta-function distributions of neutron star and black hole masses(Thorsett & Chakrabarty 1999) but is now confirmed by more accurate observations. Supported by increasingly sophisticated simulations and these predictions, the convective engine became the leading model for most supernovae. But the real proof of this engine came from the distribution of ejecta in supernova remnants, in particular the distribution of the ^{44}Ti in the Cassiopeia A supernova remnant(Grefenstette et al. 2014, 2017).

One of the leading alternative engines for supernovae invokes magnetic fields, either in a disk around the proto-neutron star or a strongly magnetized PNS. This engine taps the rotational energy in the collapse and requires a rapidly rotating stellar core. It has, as yet, little predictive power, but within the broad uncertainties of this class of engines, it is possible to produce an explosion. We can derive the requirements on the core rotation for such engines. For disk models, there must be enough angular momentum to form a disk around the 30 km PNS. For centrifugal support,

$$\frac{v_{\rm rot}^2}{r_{\rm disk}} = \frac{j_{\rm rot}^2}{r_{\rm disk}^3} = \frac{GM_{\rm PNS}}{r_{\rm disk}^2} \tag{1}$$

where $j_{\rm disk} = v_{\rm rot} r_{\rm disk}$ is the angular momentum in a disk of radius $r_{\rm disk}$, G is the gravitational constant, and $M_{\rm PNS}$ is the PNS mass. For a $1.4\,M_\odot$ PNS and a disk of 100 km requires an angular momentum above the PNS of $2.4\times10^{16}\,{\rm cm^2\,s^{-1}}$. Similarly, for a rotating magnetar model to have sufficient energy, the PNS must have sufficient rotational energy to drive an explosion:

$$E_{\rm rot} = \frac{1}{2} I\omega^2 = \frac{1}{2}\frac{J^2}{I} \tag{2}$$

where $I \approx 2/5 M R_{\rm PNS}^2$. Again, for a 10^{51}erg explosion, the magnetar engine requires specific angular momenta $j \approx 4\times10^{15}\,{\rm cm^2\,S^{-1}}$. This engine is akin to the collapsar engine for gamma-ray bursts(Woosley 1993) that invoked an accretion disk around a black hole to explain long-duration gamma-ray bursts. Since the specific angular momentum of a star in-

creases with radius, the total stellar spin requirements for this gamma-ray burst engine are not as extreme as the alternative supernova engine. Even so, it is believed only to be produced in specific evolutionary scenarios where the star was spun up through binary interactions(Fryer et al. 2007).

In these engines, gravitational waves are produced both during the core bounce and the convection both within and just above the newly-formed neutron star. Sources that are strongest during the bounce include asymmetric collapse and rotational collapse. Convection within and just above the newly-formed neutron star produces gravitational waves that begin after the bounce over a timescale dependent on the growth time of these convective instabilities. In this section, we review all of these sources, focusing on distinguishing features of each source.

The gravitational wave signal from stellar collapse has now been studied extensively (for a review, seeFryer & New (2003, 2011)), with a wide range of modelsMoenchmeyer et al. (1991); Fryer et al. (2002); Fryer & Warren (2004); Müller et al. (2004); Fryer et al. (2004); Kotake et al. (2011); Takiwaki & Kotake (2011); Ott et al. (2012, 2013); Abdikamalov et al. (2014); Yokozawa et al. (2015); Hayama et al. (2016); Richers et al. (2017) varying the characteristics of the progenitor (density, entropy, angular momentum profiles), density perturbations in the pre-collapse model, and input physics (e.g. equation of state). The basic properties in the signals that persist throughout all simulations are as follows:

- The amplitude of the gravitational wave signal is roughly 10^{-22} at 10 kpc for non-rotating models up to 10^{-20} at 10 kpc for the fastest rotating progenitors. The amplitude for strongly asymmetric collapses is roughly 10^{-21} at 10 kpc.
- The highest amplitude signal from rotating stars or asymmetric collapses exists only for 1-2 cycles, after which the amplitude is drops dramatically, typically down to $1-5\times10^{-22}$ at 10 kpc (slightly higher than non-rotating models).
- The onset of the gravitational wave signal for models dominated by entropy-driven convection will begin shortly after bounce and grow with time. For convection dominated by the standing accretion shock instability, there is a delay (100 – 200 ms) between bounce and the onset of the gravitational wave signal.
- The frequency of the instability peaks around 100-1000Hz. Although there is some evidence that the frequency might decrease as the size of the convective region increases, there is not a fixed quantitative evolution and no reliable templates exist.

The existence of a large initial gravitational wave signal is a strong indication of high rotation. It is characterized by a very large amplitude cycle followed by weaker amplitude (by over an order of magnitude) until the launch of the explosion. Asymmetric collapse can produce very strong amplitudes as well and these high amplitudes are likely to last 2-3 cycles before damping out. In this way, it may be possible to distinguish between highly rotating and asymmetric collapses. But more asymmetric collapse calculations are required to confirm these comparisons. Supernova engines that require high rotation (e.g. magnetic-driven engines) can be ruled out in collapse models where this signal feature is not observed.

Slow-rotating systems (considered more likely based on the birth spin values of neutron stars) will produce much weaker signals. The delay between the bounce neutrinos and the GW signal provides a gauge of the growth of the convection. If Rayleigh-Taylor convection is weak, there will be a delay ($\sim$ 100 ms) in the GW signal as the standing accretion shock instability grows. If Rayleigh-Taylor is strong, the GW signal will begin shortly after the neutrino signal. For systems close enough to observe GWs from convection, a measurement can help constrain the nature of the supernova engine.

The cores of stars with very fast rotation can develop bar modes and even fragment (see Fryer et al. (2004); Fryer & New (2011) for reviews) that will have very strong signals that may be observed well beyond the Milky Way.

3. TOY MODEL OF SUPERNOVA GRAVITATIONAL WAVES

What would work here for detection. What we can really say for sure is that the frequency of the oscillations typically peaks at the 100-1000Hz region. But it will not be uniform (no exact template like for compact object mergers). I discuss some of the features of different models above.

Doing HD modeling or solving the stellar structure during SN is complicated, but we can make a simplified toy model that to 0^{th} order captures the relevant physics that allow us to estimate the expected signal to be observed in the LIGO or the next generation detectors. In addition it is possible to learn about the SN engine that generated the GW signal, the signals' duration, magnitude, and dissipation with distance.

4. THE SUPERNOVA RATE OF THE SOLAR NEIGHBORHOOD

Determining the supernova rate in the volume around the Sun, i.e. the solar neighborhood, has been done from using numerous different data sources. In this section we scan the literature on solar neighborhood SN rates and present the different obtained results in a homogeneous and coherent manner. In order to compare across different data sources we define the SN rate as the SN surface density in units of $\mathrm{kpc^2 Myr^{-1}}$.

4.1. *Historical Supernovae*

Table 1. The known historical SNe known to have happened since yr 1000 AD, with year, distance, galactic latitude and galactic longitude.

SN name	year (AD)	distance (kpc)	l (°)	b (°)	type	ref.*
Lupus SN	1006	2.2	327.57	14.57	Ia	1
Crab	1054	2.0	184.55	-5.79	II	1
3C 58	1181	2.6	130.73	3.07	II	1
Tycho	1572	2.4	120.09	1.42	Ia	1
Keplers'	1604	4.2	4.53	6.82	Ib/II	1
Cas A	1680	2.92	111.73	-2.13	Ib	1
MSH 54-11	>1000	3.0	259.78	1.69	II/Ib	2

∗: 1: The et al. (2006) 2: Dragicevich et al. (1999)

Since 1000 AD 7 SN remnants (SNR) within 5 kpc of the Sun has been discovered. Of these, 5 where observed as a new star on the sky and recorded in to the log books of astronomers across different cultures (Dragicevich et al. 1999). In Tabel 4.1 are shown the name, year AD of SN, galactic latitude and longitude, and SN type of these 7 SNR. In Fig. 1 we have added the position of each SNR in the MW as orange dots.

The SN rate in the solar neighborhood out to 5 kpc from the historical record is $7/(\pi 5^2 \mathrm{kpc}^2 0.001\mathrm{Myr}) = 89\mathrm{kpc}^2\mathrm{Myr}^{-1}$.

4.2. *Goulds' Belt*

The EGRET satellite observed numerous unknown persistent point sources at medium latitude. These were identified by Grenier (2000) to be formed in the star burst region Goulds' belt that surrounds the Sun and indicates a history rich in SNe. Given that the belt currently houses 432 ± 15 SN progenitors Grenier (2000) estimated that recently the belt gave rise to a local SN frequency of 20-27 SN Myr^{-1} and a SN rate of 75-95 kpc^{-2} Myr^{-1}.

4.3. *Geological record*

SNR are believed to be the birth sites of cosmic rays which impinges Earths' atmosphere to produce radioactive isotopes such as ^{14}C and ^{10}Be which are used as proxies for age determination and the terrestrial climate. If the SN rate changes, so does the number of SNR and the influx of cosmic rays on Earth and hence also the production of ^{14}C and ^{10}Be. Analysis of the time series of ^{14}C and ^{10}Be 300 kyr back in time suggests that 23 SN exploded within 300 pc of the Sun (Firestone 2014). The solar neighborhood SN rate from this study is $23/(\pi 0.3^2 \mathrm{kpc}^2 0.3\mathrm{Myr}) = 271\mathrm{kpc}^2\mathrm{Myr}^{-1}$.

Search the literature for estimates of the supernova rate in the solar neighborhood. Discuss, what are the available data sources, what are the estimates made from these sources, and how do they compare to each other - consistency across data sources or not? Do the local Galactic structure play a role in the local SN rate in the recent past ∼1Myr or not?

- historical SN
- O-type stars
- C-14 and Be10
- EGRET unidentified persistent γ-ray sources.
- ...

5. FREQUENCY OF SUPERNOVAE IN THE MILKY WAY

The overall SN frequency of the MW can be estimated in a number of ways using different data sources. We will focus on three different data sources in this section, i) extra-galactic surveys, ii) MW stellar end-product data, and iii) Historical record. In table 5.1 we summarize the MW SN frequency from a number of different data records. Where applicable we also use different values of the Hubble constant H_0. The remainder of this section describes the

5.1. *SN frequencies from extra-galactic surveys*

The opportunity to observed a SN in the MW or even in the nearest galaxies like the Megallanic clouds or Andromeda, is rare. However, looking at a large sample of galaxies allows SNe to be observed frequently. Proper statistical treatment of the galaxy sample and its completeness, makes it possible to, infer the rate of SN for different galaxy- and SN types. The extra-galactic SN surveys measures the relative SN rate of each galaxy- and SN type in SN units (SNu) which is the SN frequency scaled with the dimensionless Hubble parameter h^2 and the B-band or blue luminosity $L(B)$ of the galaxy, in units of $10^10 L_\odot$. The transformation from SNu to MW SN frequency ν then is

$$\nu = SNu \left(\frac{H_0}{100 \frac{km}{sMpc}} \right)^2 \left(\frac{L(B)}{10^{10} L_\odot} \right) \frac{1}{100\mathrm{yr}} \qquad (3)$$

where H_0 is the Hubble constant and $L(B)$ is the MW blue luminosity. Note that $h = \frac{H_0}{100 \frac{km}{sMpc}}$ is the Hubble parameter. Because, estimates of the Hubble constant falls into two distinct regimes inconsistent with each other, we adopt here three different values of the Hubble constant $H_{0,[1,2,3]}$. $H_{0,1} = 75$km s^{-1} Mpc^{-1} is adopted for historical reasons, as it has been the value used in most extragalactic surveys to estimate the MW SN frequency. Both $H_{0,2}$ and $H_{0,3}$ are more recent estimates. $H_{0,2} = 67.8 \pm 0.9$km s^{-1} Mpc^{-1} is taken from Planck Collaboration et al. (2016) and $H_{0,3} = 73.24 \pm 1.7$km s^{-1} Mpc^{-1} from Riess et al. (2016). Using $H_{0,1}$ thus systematically overestimate the MW SN frequency, which compared to $H_{0,2}$ yields a

Table 2. Solar neighborhood SN rates

Method	SN rate (kpc^{-2} Myr^{-1})	ref.
Historic SN	89	Dragicevich et al. (1999)
SN progenitors	75-95	Grenier (2000)
Atmospheric ^{14}C and ^{10}Be	271	Firestone (2014)
OB type stars $D \leq 0.6$kpc	18.5 ± 4	Hohle et al. (2010)
OB type stars $D \leq 5$kpc	1.4 ± 0.2 (70 ± 10)	Schmidt et al. (2014)

difference of $\sim 20\%$. For a review on the early development of extra-galactic SN surveys, methods, and earliest estimated rates we refer to van den Bergh & Tammann (1991). The 5 surveys of Muller et al. (1992); Cappellaro et al. (1993); van den Bergh (1993); Tammann (1994); Cappellaro et al. (1997), rows 1-5 in table 5.1 respectively, are summarized in Dragicevich et al. (1999). We thus concentrate on extragalactic surveys not included in Dragicevich et al. (1999).

Cappellaro et al. (1999) repeated their 1997-study (Cappellaro et al. 1997), with an extended time series of Evans' visual SN survey to include data from 1980 - 1998. Bias correction was done as described in Cappellaro et al. (1997). The increased number of SNe detections made by Evans gives a more complete sample and overall a better estimate is obtained with the extended data sample compared to the previous 1997-study, row 5 in tab. 5.1.

The Lick Observatory supernova search (LOSS) is described in a series of papers Leaman et al. (2011); Li et al. (2011b,a, LOSS papers) and is the result of a SN search campaign using a fully robotic telescope. It is, to date, the most successful of the SN search campaigns owing to its large data base of SNe approaching 1000 SNe detections across nearly 15000 galaxies. Their estimated MW SN frequency is based on the LOSS *optimal* galaxy sample, which excludes the small (major axis <1 arcmin) E and S0 galaxies. Further this sample excludes highly inclined ($i > 75^\circ$) spiral galaxies. A complete SN sample also constructed introducing a cut-off distance of 80 Mpc for SN type Ia and 60 Mpc for types Ibc and II. The LOSS papers adopts the WMAP Hubble constant, $H_0 = 73$ km s^{-1} Mpc^{-1}, from Spergel et al. (2007). The mean MW SN frequency from the seven extragalactic SN surveys, for the three Hubble constants are $\nu_{h_1} = 2.78$ 100yr $^{-1}$, $\nu_{h_2} = 2.27$ 100yr $^{-1}$, $\nu_{h_3} = 2.63$ 100yr $^{-1}$, respectively.

6. COMPARING SUPERNOVA RATE OF THE MILKY WAY TO THE SOLAR NEIGHBORHOOD

When we convert estimates of the MW SN frequency into SN rates close to the Sun and compare to the SN rate from observations within 5 kpc of the Sun these are not coherent. An often discussed cause for this discrepancy between the two different data sources is the current position of the Sun within the MW. Supposedly we are in a special place in the MW. Indeed, some interesting environmental features related to formation of massive stars are found fairly close to Sun. Most notably are the local bubble and Goulds' Belt which the Sun is currently setting within. The local bubble is believed to be the product of several SNe within the past few Myr (cite). Goulds' belt is a much bigger structure with a radius of 300 pc believed to have produced a SN rate 3-5 times that of the *normal* SN rate during the last 40 Myr (cite). Finally, somewhat further away are the spiral arms Carina-Sagittarius and Perseus (cite) which are the birth place of many stars including CCSN progenitors. Such features around the Sun indicates the MW stellar disc is non-axis-symmetric and have local fluctuations in the SN rate that when averaged out to entire MW disc is coherent with SN frequencies from extra galactic surveys reviewed in 5. To test the hypothesis that the position of the Sun in the MW can make coherence between our local SN rate and the MW SN frequency it is necessary to model the MW SN distribution.

6.1. *Modeling the Milky Way supernova distribution*

As was seen in our review of MW SN frequency and in particular those including the historical record of SNe assumes the MW to be axis-symmetric which it is not. It is well established that of non-axis-symmetric components are 4 spiral arms which are correlated with regions of free electrons, star formation, and pulsars (Shaviv 2003; Taylor & Cordes 1993; Faucher-Giguère & Kaspi 2006). Here we model the MW CCSNe distribution taking into account the MW spiral structure. Our aim is to compare solar neighborhood SNe rates with that of the MW SN frequency.

Ideally we should take into account SN types, and some spread due to BSS and DES effects, see Eldridge, Langer, Tout 2011. Finally, we should allow type Ia to be spread homogeneous in the MW.

Given a Milky Way SN frequency we estimate the corresponding local SN rate, i.e. the number of SN in time and space out to some distance from the Sun.

The simulation is limited in time to 1 Myr such that we avoid having to account for dynamics of stars, chemical evolution, and interactions of the Milky Way with the

Table 3. MW SN frequencies from extra-galactic SN rate surveys. Column presents the source of data. Columns 2-4 gives the MW SN frequency of each survey for different Hubble parameters $h_{1,2,3}$, and column fives gives the reference to each survey. Hubble parameter $h_1 = 0.75$ is a typically used value, see Dragicevich et al. (1999), $h_2 = 0.678 \pm 0.009$ is taken from the Planck Satellite (Planck Collaboration et al. 2016), while $h_3 = 0.7324 \pm 0.017$ is from Riess et al. (2016).

	Method	MW SN frequency			source
		h_1	h_2	h_3	
1	Berkeley (CCD)	4.0 ± 2.0	3.2 ± 1.6	3.8 ± 1.9	Muller et al. (1992)
2	Asiago and Sternberg (photographic)	2.0 ± 1.1	1.6± 0.8	1.9 ± 1.0	Cappellaro et al. (1993)
3	Evans (Visual)	3.0 ± 1.5	2.4±1.2	2.8 ± 1.4	van den Bergh (1993)
4	Distance-limited galaxies	≈4.7	3.8	4.4	Tammann (1994)
5	Combining 4 photographic and 1 visual (1980-89)	1.3 ± 0.9	1.0±0.7	1.2±0.8	Cappellaro et al. (1997)
6	Combining 4 photographic and 1 visual (1980-98)	1.49 ± 0.44	1.21±0.35	1.42±0.41	Cappellaro et al. (1999)
7	Lick Observatory Supernova Search	2.99 ± 0.63	2.44±0.51	2.85±0.60	Leaman et al. (2011); Li et al. (2011b,a)

LMC/SMC as suggested by Shaviv (2003). It is further assumed that the MW star formation rate is constant over this period hence the MW SN frequency is also constant during this time.

The CCSN will be positioned according to a model of the birth sites of pulsars which we model with three components. First is the radial distribution from Yusifov & Küçük (2004) which is given as

$$\rho(r) = A \left(\frac{r+R}{R_\odot + R_1} \right)^a \exp\left[-b \left(\frac{r-R_\odot}{R_\odot + R_1} \right) \right] \quad (4)$$

where $\rho(r)$ is the surface density at Galacto-centric radius r. The model parameters and their respective value are A=36.7 ± 1.9 kpc^{-2} , R_1 = 0.55±0.1, a=1.64±0.11, and b = 4.01 ± 0.24. This distribution from Yusifov & Küçük (2004) actually is a fit to the evolved pulsars population in the MW not their birth site. However, as argued by Faucher-Giguère & Kaspi (2006) observations of pulsars is biased towards young pulsars which is correlated with regions of star formation and supernovae. Hence, eq. (4) is likely to describes well the radial surface density of SNe in the MW. Besides a concentration of CCSN towards the MW center, CCSN are also correlated with the MW spiral arms which is the second component of our model.

The MW spiral arm structure is modeled following the model of Wainscoat et al. (1992) in which there are 4 arm centroids, the loci of which is analytically described by

$$\theta(r) = k \ln(r/r_0) + \theta_0 \, . \quad (5)$$

The values of each arm is given in Table 4 and are taken from Faucher-Giguère & Kaspi (2006) who adopted a different coordinate system than Wainscoat et al. (1992).

Finally the third component is the spread of CCSN below and above the MW plane in the z-direction. We model the z distribution as a exponential surface density

$$\sigma_z(z) = \exp(-z/H_z) \quad (6)$$

Table 4. Parameters of the spiral arms

Arm number	Name	k(rad)	r_0(kpc)	θ_0 (rad)
1	Norma	4.25	3.48	1.57
2	Carina-Sagittaurius	4.25	3.48	4.71
3	Perseus	4.89	4.90	4.09
4	Crux-Scutum	4.89	4.90	0.95

where the H_z = 0.3 kpc is the scale length.

The number of MW CCSN is given as

$$N_{SN} = 10^4 \left(\frac{f_{SN}}{100yr} \right) \left(\frac{\Delta t}{Myr} \right) \quad (7)$$

where f_{SN} in units 100yr^{-1} is the MW SN frequency and Δt is the time period over which we simulate in units of Myr.

Each SN is assigned a position in cylindrical coordinates (r, θ, z) by prescription following Faucher-Giguère & Kaspi (2006) which is described below. First we select with equal probability a spiral arm i = [1,2,3,4] assuming an equal birth rate in each arm. Secondly, we drawn a distance r_{raw} from eq. (4) and the corresponding polar angle θ_{raw} is calculated using eq. 5 such that the SN lies on the i^{th} arms' centroid. The polar angle is corrected to avoid artificial features near the MW center by adding a correction of magnitude $\theta_{corr} \exp(-0.35 r_{raw}/kpc)$, where θ_{corr} is uniformly chosen in the interval [0;2π[rad. To spread out the SNe around the spiral arm centroids, we alter the (x,y) coordinates of each SN as $(x + x_{corr}, y + y_{corr})$ where $(x_{corr}, y_{corr}) = (r_{corr}\cos(\theta), r_{corr}\cos(\theta))$. Here r_{corr} is drawn from the a normal standard deviate with with a mean of zero and standard deviation $0.07 r_{raw}$.

In Fig. 1 is shown an example of our MW CCSNe model over the a 1 Myr period. We show the distribution in the MW (r,z)-plane in top panel. With increasing radius from the MW center the mean distance from the plane of CCSN

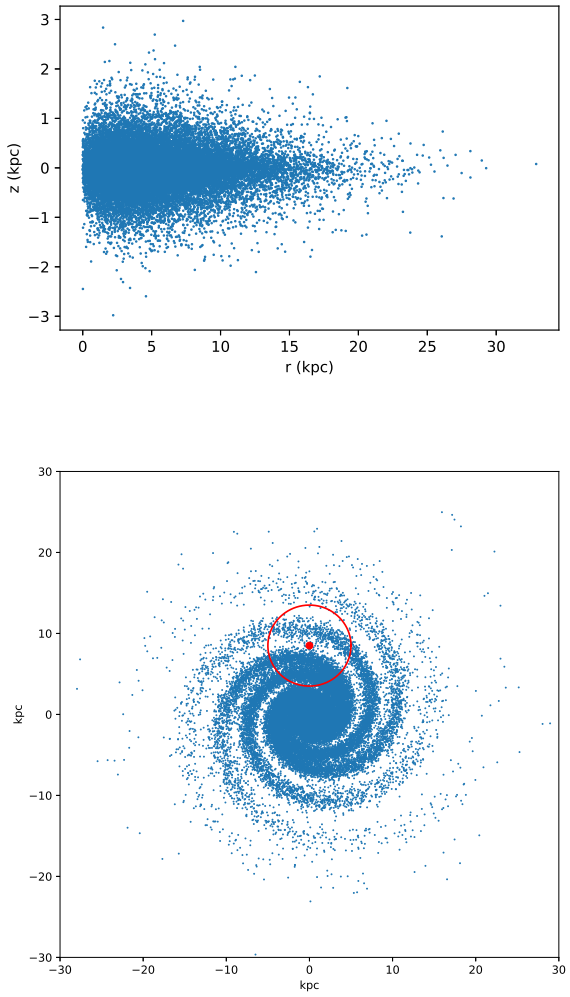

Figure 1. The distribution of CCSN in the MW. Top panel shows the distribution in the MW (r,z)-plane and the lower panel shows the distribution in the MW (x,y)-plane. **Top:** The larger radial concentration automatically ensures a larger spread in the z-direction close to the MW center. **Lower:** The spiral structure of the MW is clearly visible. Drawn into the figure is the Suns' position and a circle of radius 5 kpc centered on the Sun.

decreases which in consequence of the higher concentration of CCSN in the MW inner region. The lower panel shows the distribution of CCSN in the MW (x,y)-plane where the imprints of the spiral arm structure is clearly seen. Marked as a red dot is the Sun and centered on it is a circle of 5 kpc.

6.2. *Our Monte Carlo simulation*

Given our model of CCSN in the MW we set up a Monte Carlo (MC) simulation from which we get a statistical ensemble from which we can evaluate the coherence between local and global SN frequencies and the local SN rate. The MC simulation performs the following steps

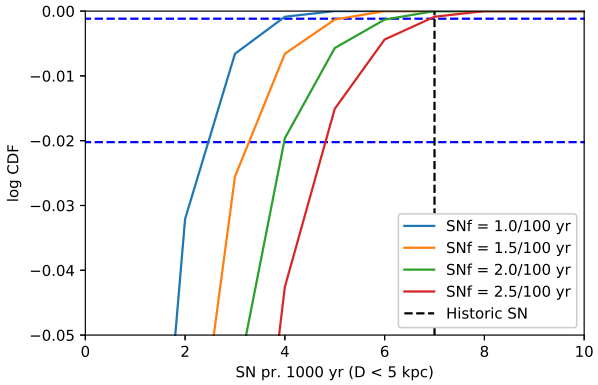

Figure 2. Cumulative probability distribution to observe a specific number of SNe within 1000 yr within 5 kpc of the Sun for different MW SN frequencies. Black dashed vertical line marks the historical observed number of SNe. Blue dashed lines each mark a 1-σ(button) and 2-σ(top).

1. Choose a global SN frequency and determine N_{SN}
2. Distribute the N_{SN} into types of SN.
3. Populate the MW with SN in space and time given their SN type.
4. Find the time series of SNe within an Euclidean distance to the Sun of 5 kpc.

With the MC simulation we create an ensemble of 10^6 samples which allows us to calculate the chance of observing n_{sn} within 5 kpc of the Sun and compare to the historical record of SN summarized in Table 4.1.

Figure 2, shows the cumulative probability distribution to observe a number of SNe within 5 kpc in a 1000 yr period, for four different MW SN frequencies, $\nu_{MW} = [1, 1.5, 2, 2.5]$. The horizontal blue lines marks the 2-σ(button) and 3-σ(top) level respectively. We can (preliminary) infer three important conclusions from this simulation, i) the number of SNe within 5 kpc within 1000 yr of the Sun follows a Poisson distribution, ii) the historical record was a rare event, more specifically, a 3-σ event if the MW SN frequeny is 2.5, and iii) if the MW SN frequency is likely not much smaller than 2.5 SN 100yr^{-1} as the probability to observe the historical record because immensely unlikely.

From our MC simulation it is also possible to estimate the waiting time between two SNe within 5 kpc of the Sun as a function of MW SN frequeny. This is depicted in Fig. 3 as the blue line. As expected the frequency is proportional to the period. The proportionality is a scaling of the relative area of SNe to explain the historical record over the total MW area. Though, the median waiting time for a SN within 5kpc assuming a MW SN frequency of 2.5 100yr^{-1} is over due, it

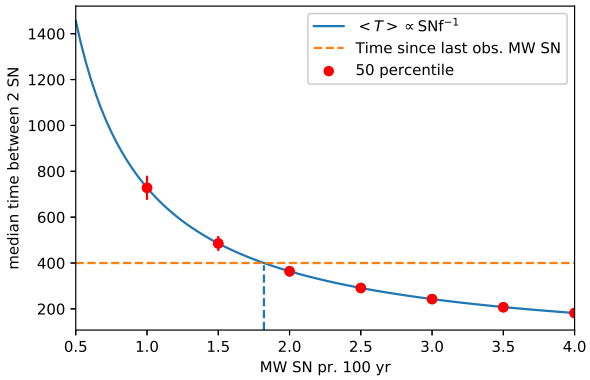

Figure 3. Median time between two SN within 5 kpc of the Sun as a function of MW SN Frequency, blue line. Horizontal dashed line marks the current approximate time since the last SN within 5kpc of the Sun. The vertical dashed line marks the MW SN frequency corresponding to a median waiting time of 400 yr.

is likely not in real conflict the historical record, but a matter of statistical fluctuations.

7. THE RATE OF SUPERNOVA GRAVITATIONAL WAVE SIGNALS

When comparing the rates of supernova near the Sun and in the MW with the (potential) distance limitation due to the /relative weak/small) GW signal of a SN how many observations could one expect to be observed with LIGO and the next generation observations? If problematic for LIGO and next generation detectors, what is needed for future detector designs to comply with our estimated rate?

8. WHY WE OBSERVED A SN BUT NO GW SIGNAL WITH IT?

9. DISCUSSIONS

10. CONCLUSIONS

11. SUMMARY

Summary text.

Acknowledgments.

Facilities: facility ID, facility ID, facility ID

Software: Numpy

REFERENCES

Abdikamalov, E., Gossan, S., DeMaio, A. M., & Ott, C. D. 2014, PhRvD, 90, 044001

Cappellaro, E., Evans, R., & Turatto, M. 1999, A&A, 351, 459

Cappellaro, E., Turatto, M., Benetti, S., et al. 1993, A&A, 273, 383

Cappellaro, E., Turatto, M., Tsvetkov, D. Y., et al. 1997, A&A, 322, 431

Dragicevich, P. M., Blair, D. G., & Burman, R. R. 1999, MNRAS, 302, 693

Faucher-Giguère, C.-A., & Kaspi, V. M. 2006, ApJ, 643, 332

Firestone, R. B. 2014, ApJ, 789, 29

Fryer, C. L. 1999, ApJ, 522, 413

Fryer, C. L., Holz, D. E., & Hughes, S. A. 2002, ApJ, 565, 430

—. 2004, ApJ, 609, 288

Fryer, C. L., & Kalogera, V. 2001, ApJ, 554, 548

Fryer, C. L., & New, K. C. B. 2003, Living Reviews in Relativity, 6, 2

—. 2011, Living Reviews in Relativity, 14, 1

Fryer, C. L., & Warren, M. S. 2004, ApJ, 601, 391

Fryer, C. L., Mazzali, P. A., Prochaska, J., et al. 2007, PASP, 119, 1211

Grefenstette, B. W., Harrison, F. A., Boggs, S. E., et al. 2014, Nature, 506, 339

Grefenstette, B. W., Fryer, C. L., Harrison, F. A., et al. 2017, ApJ, 834, 19

Grenier, I. A. 2000, A&A, 364, L93

Hamuy, M. 2003, ApJ, 582, 905

Hayama, K., Kuroda, T., Nakamura, K., & Yamada, S. 2016, Physical Review Letters, 116, 151102

Herant, M., Benz, W., Hix, W. R., Fryer, C. L., & Colgate, S. A. 1994, ApJ, 435, 339

Hohle, M. M., Neuhäuser, R., & Schutz, B. F. 2010, Astronomische Nachrichten, 331, 349

Kotake, K., Iwakami-Nakano, W., & Ohnishi, N. 2011, ApJ, 736, 124

Leaman, J., Li, W., Chornock, R., & Filippenko, A. V. 2011, MNRAS, 412, 1419

Li, W., Chornock, R., Leaman, J., et al. 2011a, MNRAS, 412, 1473

Li, W., Leaman, J., Chornock, R., et al. 2011b, MNRAS, 412, 1441

Moenchmeyer, R., Schaefer, G., Mueller, E., & Kates, R. E. 1991, A&A, 246, 417

Müller, E., Rampp, M., Buras, R., Janka, H.-T., & Shoemaker, D. H. 2004, ApJ, 603, 221

Muller, R. A., Newberg, H. J. M., Pennypacker, C. R., et al. 1992, ApJL, 384, L9

Ott, C. D., Abdikamalov, E., Mösta, P., et al. 2013, ApJ, 768, 115

Ott, C. D., Abdikamalov, E., O'Connor, E., et al. 2012, PhRvD, 86, 024026

Planck Collaboration, Ade, P. A. R., Aghanim, N., et al. 2016, A&A, 594, A13

Richers, S., Ott, C. D., Abdikamalov, E., & O'Connor, E. a nd Sullivan, C. 2017, PhRvD, 95, 063019

Riess, A. G., Macri, L. M., Hoffmann, S. L., et al. 2016, ApJ, 826, 56

Schmidt, J. G., Hohle, M. M., & Neuhäuser, R. 2014, Astronomische Nachrichten, 335, 935

Shaviv, N. J. 2003, NewA, 8, 39

Smartt, S. J. 2009, ARA&A, 47, 63

Spergel, D. N., Bean, R., Doré, O., et al. 2007, ApJS, 170, 377

Takiwaki, T., & Kotake, K. 2011, ApJ, 743, 30

Tammann, G. A. 1994, in Supernovae, ed. S. A. Bludman, R. Mochkovitch, & J. Zinn-Justin, 1

Taylor, J. H., & Cordes, J. M. 1993, ApJ, 411, 674

The, L.-S., Clayton, D. D., Diehl, R., et al. 2006, A&A, 450, 1037

Thorsett, S. E., & Chakrabarty, D. 1999, ApJ, 512, 288

van den Bergh, S. 1993, Comments on Astrophysics, 17, 125

van den Bergh, S., & Tammann, G. A. 1991, ARA&A, 29, 363

Wainscoat, R. J., Cohen, M., Volk, K., Walker, H. J., & Schwartz, D. E. 1992, ApJS, 83, 111

Woosley, S. E. 1993, ApJ, 405, 273

Yokozawa, T., Asano, M., Kayano, T., et al. 2015, ApJ, 811, 86

Yusifov, I., & Küçük, I. 2004, A&A, 422, 545